27
5-30-79

ANL/MSD-79-2

ANL/MSD-79-2

MASTER

NONDESTRUCTIVE EVALUATION TECHNIQUES FOR HIGH-TEMPERATURE CERAMIC COMPONENTS

Sixth Quarterly Report

January—March 1979

U of C-AUA-USDOE

ARGONNE NATIONAL LABORATORY, ARGONNE, ILLINOIS

Prepared for the U. S. DEPARTMENT OF ENERGY
under Contract W-31-109-Eng-38

DISCLAIMER

ANL/MSD-79-2

ARGONNE NATIONAL LABORATORY
9700 South Cass Avenue
Argonne, Illinois 60439

NONDESTRUCTIVE EVALUATION TECHNIQUES FOR HIGH-TEMPERATURE CERAMIC COMPONENTS

Sixth Quarterly Report
January-March 1979

Materials Science Division

April 1979

THIS PAGE

WAS INTENTIONALLY

LEFT BLANK

TABLE OF CONTENTS

LIST OF FIGURES

HIGHLIGHTS

An example is presented which demonstrates the advantage of dye-enhanced radiographic techniques over conventional radiography for surface flaw detection. In another example, acoustic-microscopy techniques are used to reveal the presence of a small (100 x 50 μm) crack-like flaw not detectable by other techniques. Progress in the development of systems for helically scanning SiC tubing, employing acoustic-microscopy techniques and using conventional ultrasonic techniques from the bore side, is discussed.

NONDESTRUCTIVE EVALUATION TECHNIQUES FOR HIGH-TEMPERATURE CERAMIC COMPONENTS SIXTH QUARTERLY REPORT JANUARY-MARCH 1979

D.S. Kupperman, N. Lapinski, and D. Yuhas*

I. INTRODUCTION

High-temperature ceramic components are of particular interest because they are lighter than their metallic counterparts, have good corrosion resistance, and can be fabricated from inexpensive and abundant elements. As a result, the use of these ceramics can lead to more efficient energy-conversion systems.

In recent years, significant progress has been made in the use of ceramics for structural applications. Silicon carbide (SiC), for example, is currently being used for heat-exchanger tubing because of its excellent thermal-shock resistance, low coefficient of expansion, high thermal conductivity and strength at high temperature.

The reliable use of ceramics as structural components, however, requires effective failure prediction and thus effective flaw-detection capabilities. The lifetime of SiC components is affected by cracks, porosity, inclusions and free silicon. The size of critical cracks leading to fracture can be relatively small (an order of magnitude or more smaller than in comparable metallic parts) and related to microstructural features such as grain size. Many fracture origins are adjacent to the surface[1], indicating that surface cracks are an important cause of failure. Nondestructive evaluation (NDE) techniques that are satisfactory for metals may not be for ceramics. Depending on the component of interest, it may be necessary to develop or advance conventional NDE techniques for ceramic applications. Currently, the techniques most widely employed by industry for ceramic NDE are x-radiography and fluorescent dye penetrant testing. However, efforts are under way at several institutions to advance NDE techniques for structural ceramics. These techniques include high-frequency (> 50 MHz) ultrasonic testing[2], microfocus x-radiography[2], microwave NDE[3], acoustical surface-wave testing[4], photoacoustic spectroscopy[5], and acoustic-emission detection.[6]

The purpose of the present ceramic NDE program is to compare the effectiveness of conventional and unconventional NDE techniques for specific high-temperature ceramic components.

The present investigation encompasses many NDE techniques, concentrating on those not under extensive evaluation at other institutions. The techniques under evaluation include dye-enhanced radiography, acoustic microscopy, conventional ultrasonic testing, acoustic-emission detection, acoustic impact testing, holographic interferometry, infrared scanning,

*Sonoscan, Inc., Bensenville, IL

internal friction measurements and overload proof testing. No single technique is expected to serve as a universal detection method; several techniques will be required to thoroughly assess ceramic components. After an investigation of many NDE techniques, one or more NDE methods will be developed further for the specific ceramic components of interest. The current effort involves SiC heat exchangers; previous efforts have involved silicon nitride gas-turbine rotors.[7]

The current report discusses recent results acquired with radiographic, ultrasonic and acoustic-microscopy techniques.

II. RADIOGRAPHIC TECHNIQUES

The effectiveness of conventional x-radiography, dye-enhanced x-radiography and dye-enhanced neutron radiography techniques were compared using a hot-pressed silicon nitride bar, designated B2, with dimensions 150 x 6 x 6 mm. A Knoop indenter was employed to make three dents on one surface of the bar. Figure 1 shows the bar and photographs of the three surface flaws. The approximate dimensions (length x depth) of the dents are: B2-1, 500 x 50 μm; B2-2, 1000 x 25 μm; and B2-3, 900 x 70 μm. The depths of the dents range from 0.4 to 1.2% of the bar thickness t and can be used to compare the sensitivities of the three radiographic techniques, as shown below. The conventional x-radiographic technique utilized 50-KeV x-rays at a film-to-object distance of 100 cm, along with Type SR Kodak film. For the dye-enhanced radiography technique, a silver nitrate doping agent was used to fill the dent. The technique is described in a previous quarterly report (ANL/MSD-78-2). Care had to be exercised in removing the excess silver nitrate from the bar so that the dye was not removed from the dent.

Neutron-radiography techniques are described in Ref. 8. The principle of dye-enhanced neutron radiography is the same as for dye-enhanced x-radiography; that is, the flaw is filled with (in this case) a neutron-absorbing dye so that a shadow of the flaw can be obtained on the radiograph. A dye consisting of gadolinium nitrate, alcohol and a wetting agent was used here. The neutron-radiography facility of the CP-5 reactor at Argonne National Laboratory was employed for this test. The neutron-beam flux was 10^6 n/cm^2/s. The exposure time was $\sim$ 10 min and the film used was Kodak type M.

Only dent B2-3 (1.2% t) could be seen on the conventional x-radiograph. With dye-enhanced x-radiography, all three dents could be detected unambiguously; with dye-enhanced neutron radiography, all three dents could be seen with even greater clarity. This is expected, of course, as the contrast produced with dye-enhanced neutron radiography is much greater than that attainable with dye-enhanced x-radiography. Figure 2 shows photographs made from the radiographs. The dents are much more clearly evident in the actual radiographs. The circles show the locations of the visualized dents.

An attempt was also made to detect these flaws using conventional ultrasonic techniques. A pulse-echo mode was employed using contact and immersion transducers and a Sonic Mark III pulser-receiver. With normal-incidence 25-MHz (Aerotech) longitudinal waves, only dent B2-3 could be detected, and only by the presence of a slight but reproducible "bump" on the leading edge of the reflected backwall echo as the transducer was passed over the dent (see Fig. 3). With an immersion transducer in a water-bath mode converting 10-MHz longitudinal to 45° shear waves (giving a wavelength comparable to that of the 25-MHz longitudinal wave), dent B2-3 could be clearly resolved (Fig. 4). The other dents could not be detected unambiguously (i.e., $S/N \leq 2$).

These tests have demonstrated that dye-enhanced radiography techniques may be useful for flaw detection and characterization on surfaces not readily accessible for visual or conventional dye-penetrant examination. Both dye-enhanced x-radiography and dye-enhanced neutron radiography were shown capable of revealing surface flaws (dents) not detectable via conventional ultrasonic techniques.

III. ACOUSTIC MICROSCOPY

A hot-pressed silicon carbide bar, 150 x 6 x 6 mm, was used to compare various techniques for detection of a small (100-μm) surface flaw and illustrate the capability of acoustic microscopy. A small "crack" was introduced at the center of the bar via the Knoop indenter technique. Figure 5 shows the defect, which is ∿ 100 μm long and (assuming the crack is penny-shaped) ∿ 50 μm deep. This defect could not be detected with conventional radiography, dye-enhanced radiography, fluorescent dye-penetrant techniques, or 15-MHz 45° shear waves. It could just barely be detected with holographic interferometry. However, it could be clearly detected with the Sonoscan acoustic microscope. Figure 6 shows an acoustic micrograph of an ∿ 3 x 2-mm area of the surface of the bar, in which the defect is seen as a light area. The sound, incident from the left side of the photograph, passes through the bar and is mode converted (angle-beam shear wave to surface-skimming bulk wave) at the flaw site and backscattered (as well as Doppler shifted). The microscope electronics are adjusted to detect the mixed mode consisting of the scattered and through-transmitted waves. Figure 7 schematically shows the arrangement for obtaining the micrograph of Fig. 6.

From the separation of the fringes (∿ 31.5 μm), the velocity of the surface-skimming bulk wave can be estimated. In this case it is ∿ 7.4×10^5 cm/s, within 5% of the measured shear-wave velocity of 7.65×10^5 cm/s. This example demonstrates the ability of acoustic-microscopy techniques to visualize flaws not detectable by other means.

As a result of the success experienced with acoustic-microscopy techniques for flaw detection in ceramic components, a stage is being developed to demonstrate that silicon carbide heat-exchanger tubing can be helically scanned by means of acoustic microscopy. The stage being developed would be attached to the Sonoscan acoustic-microscope table. Figure 8 shows the arrangement for carrying out the helical scan. A lathe bed is used which allows the tube to be simultaneously rotated and translated axially under a cover slip and scanning laser beam (Fig. 9). The transducer (100 MHz) remains stationary as the tube is moved around and over it. The tube is virtually sealed at both ends and filled with water through a small tube. Water is also continuously fed to the cover slip as required. This arrangement should assure good acoustic coupling between transducer, tube wall and cover slip. As the tube is scanned, a real-time image is displaced on the CRT screen. Each acoustic micrograph will cover an ∿ 2 x 3-mm area.

IV. ULTRASONIC BORE-SIDE INSPECTION OF SiC TUBES

In the previous quarterly report (ANL/MSD-79-1), the possibility of carrying out an in-service ultrasonic bore-side inspection of silicon carbide heat-exchanger tubing was discussed. Because of the high velocity of sound and small critical flaw size in SiC, higher frequencies than are used for metal heat-exchanger tubing will be required. A system is currently being planned to establish the feasibility and adequacy of employing 20-MHz (or possibly higher-frequency) longitudinal and shear waves to inspect ceramic tubing from the bore side. Normal-incidence longitudinal waves would be employed for detection of wall thinning, delamination, voids and inclusions. Circumferential and axial mode-converted shear waves would be used to detect flaws (mainly cracks). Various types of single- and multiple-crystal probes are being considered for this test. The system for helically scanning the tube has already been acquired, and is shown in Fig. 10. The probe would be carried down the tube via the axial-drive mechanism of the vertically oriented lathe bed. The tube would be rotated simultaneously to generate the helical scan. The tube is sealed at the bottom and filled with water, which serves as the couplant. With this mechanism and an adequately designed probe, the adequacy of ultrasonic bore-side tube inspections can be assessed. Plans are being made to employ computer techniques for data acquisition and analysis of flaw signals to aid in the overall analysis of the inspection concept. Tube standards with artificial flaws will also be fabricated.

V. SUMMARY

Tests comparing the effectiveness of radiographic and conventional ultrasonic techniques have shown that dye-enhanced neutron- and x-radiography techniques are capable of revealing surface flaws (in this case, small dents in a silicon nitride bar) which cannot be revealed by conventional radiographic or ultrasonic means. These results support the idea that dye-enhanced radiography may be useful for detection of flaws on surfaces not accessible for conventional dye-penetrant examination.

A small (∿ 100 x 50-μm) "crack" was made on the surface of a hot-pressed silicon carbide bar and various techniques were used in an attempt to detect it. Dye-penetrant, ultrasonic and radiographic techniques were not capable of detecting this flaw. Holographic-interferometry methods (with the bar stressed in a four-point bending fixture) were barely adequate to reveal the presence of the flaw. However, the Sonoscan acoustic microscope was able to detect the flaw unambiguously, via mode-converted surface waves scattered backwards from the flaw.

Progress has been made in the development of a stage to be used with the acoustic microscope for demonstrating the feasibility of helically scanning SiC heat-exchanger tubing. Also, some apparatus has been acquired for demonstrating the adequacy of ultrasonic bore-side inspection of SiC tubing.

REFERENCES

1. F.F. Lange, Structural Ceramic Materials Under Development, Gas Turbine Conference and Products Show, Houston, TX, March 2-6, 1975, paper 75-GT-107.

2. A.G. Evans, G.S. Kino, P.T. Khuri-Yakub and B.R. Tittman, Failure Prediction in Structural Ceramics, Mater. Eval. 35 (4), 85 (April 1977).

3. A.J. Bohr, Microwave Techniques for Nondestructive Evaluation of Ceramics, Final Report AMMRC-CTR-77-29, SRI International, Menlo Park CA (Nov. 1977).

4. B.T. Khuri-Yakub, Acoustic Surface Wave Scattering: The Detection of Surface Cracks in Ceramics, Report SC5064-2TR, Rockwell International Science Center, Thousand Oaks, CA (Dec. 1977).

5. Y.H. Wong and R.L. Thomas, Laser Photoacoustic Techniques for NDE, ARPA/AFML Review of Progress in Quantitative NDE, Scripps Institution of Oceanography, La Jolla, CA (July 17-21, 1978).

6. A.G. Evans and M. Linzer, Failure Prediction in Structural Ceramics Using Acoustic Emission, J. Am. Ceram. Soc. 56 (11), 575 (1973).

7. D.S. Kupperman, C. Sciammarella, N.P. Lapinski, A. Sather, D. Yuhas, L. Kessler, and N.F. Fiore, Preliminary Evaluation of Several NDE Techniques for Silicon Nitride Gas-Turbine Rotors, Argonne National Laboratory Report ANL-77-89 (Jan. 1978).

8. Practical Applications of Neutron Radiography and Gauging, Harold Berger, Ed., American Society for Testing and Materials, Philadelphia, PA, ASTM STP 586 (1975).

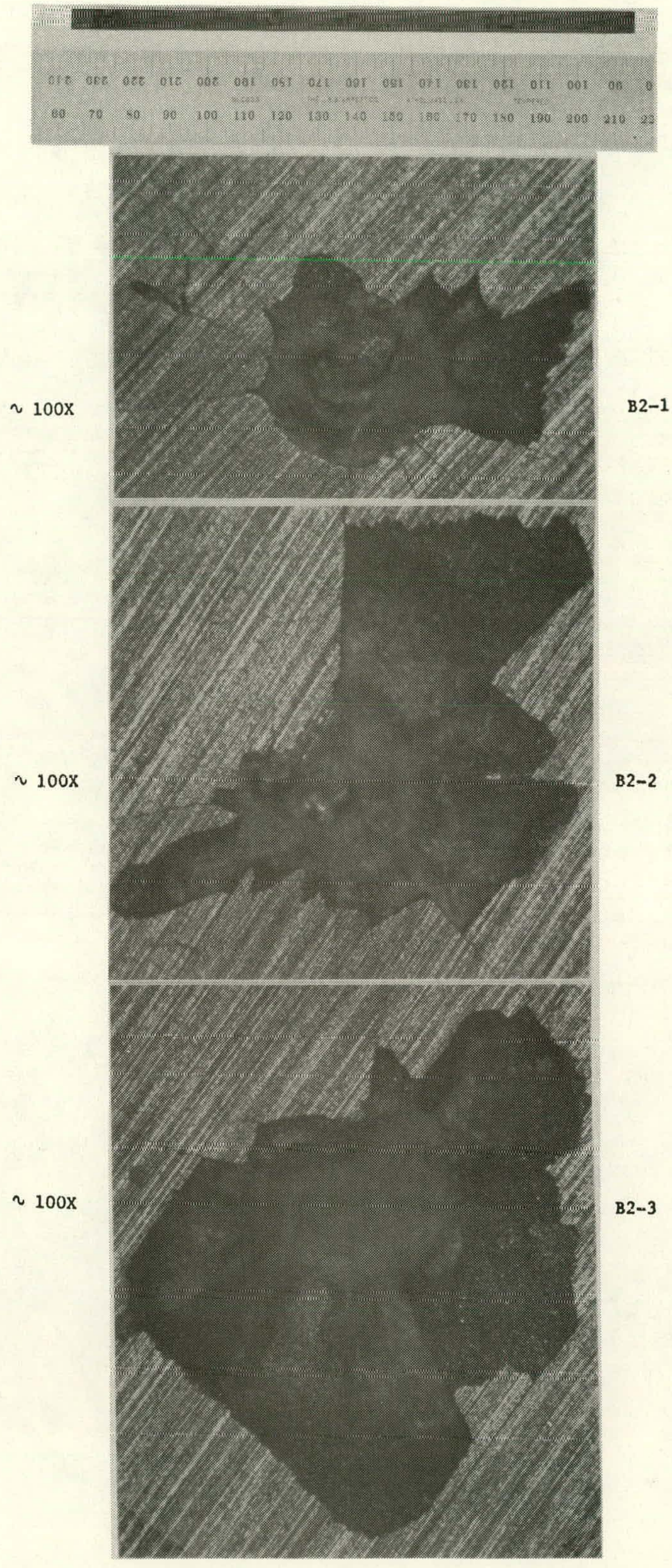

Fig. 1. Hot-pressed Silicon Nitride Bar (B2) and 100X Photographs of Three Dents Placed on One Surface of the Bar as Indicated.

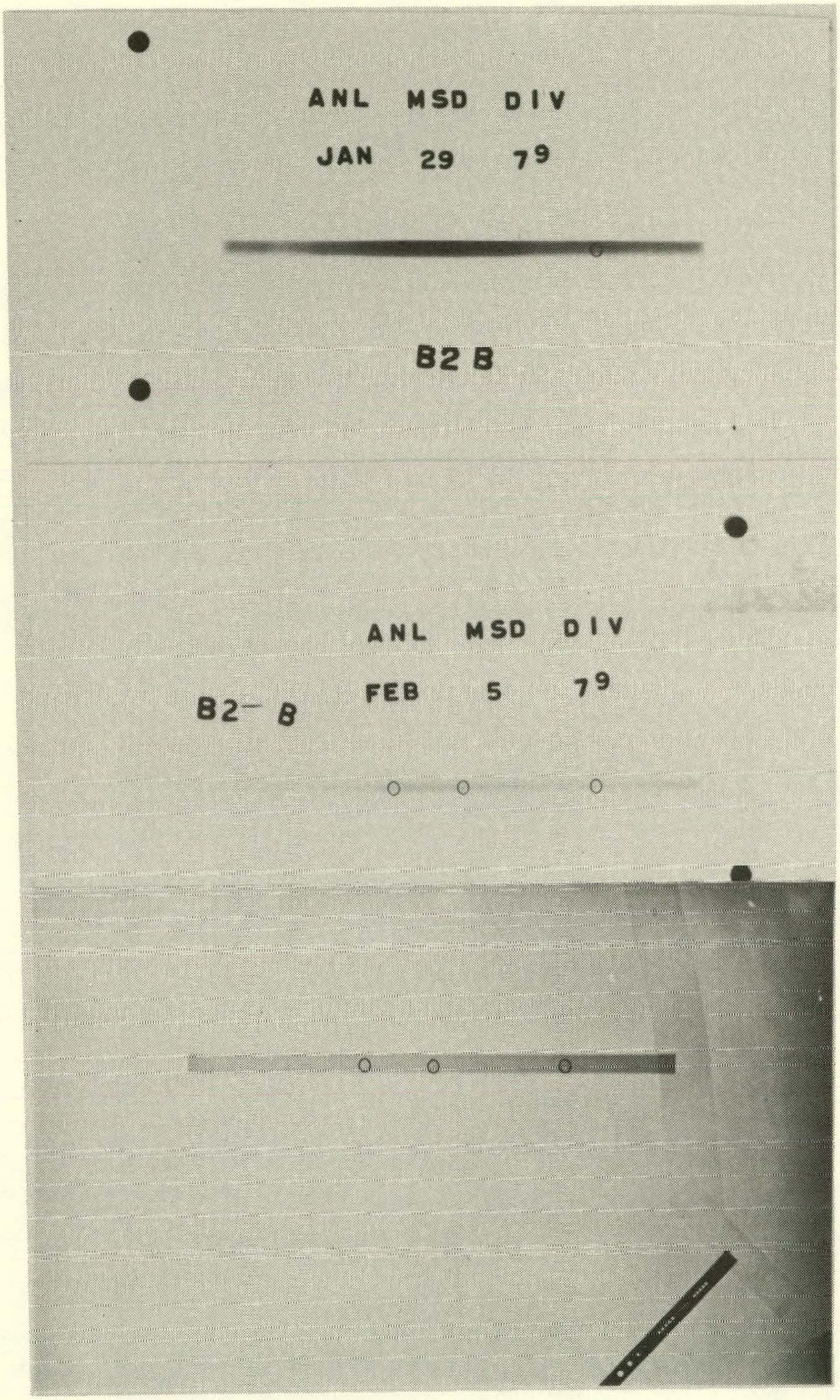

Fig. 2. Reproduction of Radiographs of Bar B2. (Top to bottom) conventional x-radiography, dye-enhanced x-radiography, and dye-enhanced n-radiography. Circles indicate locations where dents are visible in the radiographs.

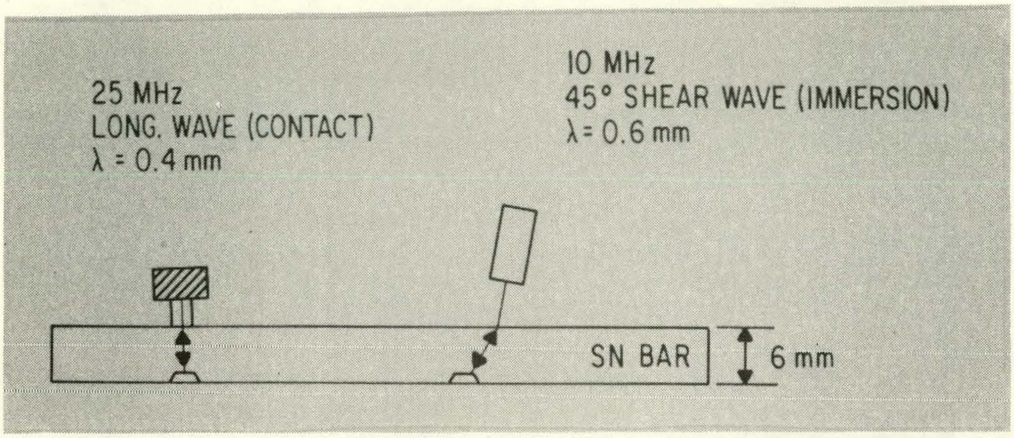

Fig. 3. Schematic Representation of Conventional Ultrasonic Method Used in an Attempt to Detect Dents in Bar B2.

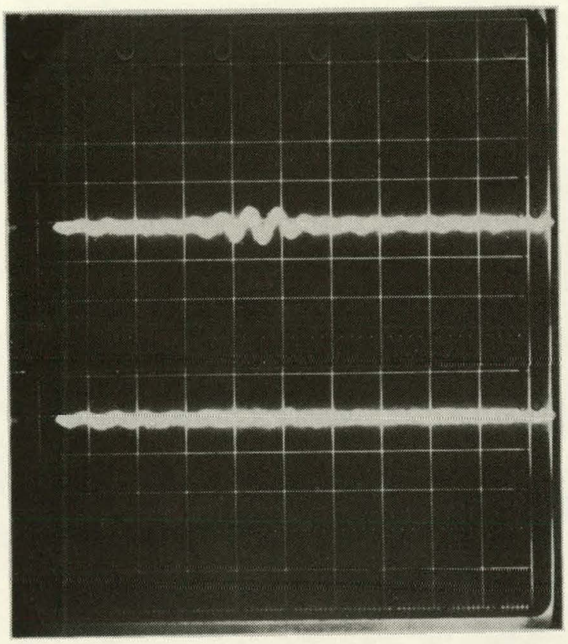

Fig. 4. Radio-frequency Traces of Ultrasonic Signals from Bar B2. 10-MHz 45° shear waves (1/2-in.-diameter immersion transducer) were used in conjunction with a Sonic Mark III pulser-receiver. (Top) echo from dent B2-3; (bottom) signal in flaw-free region.

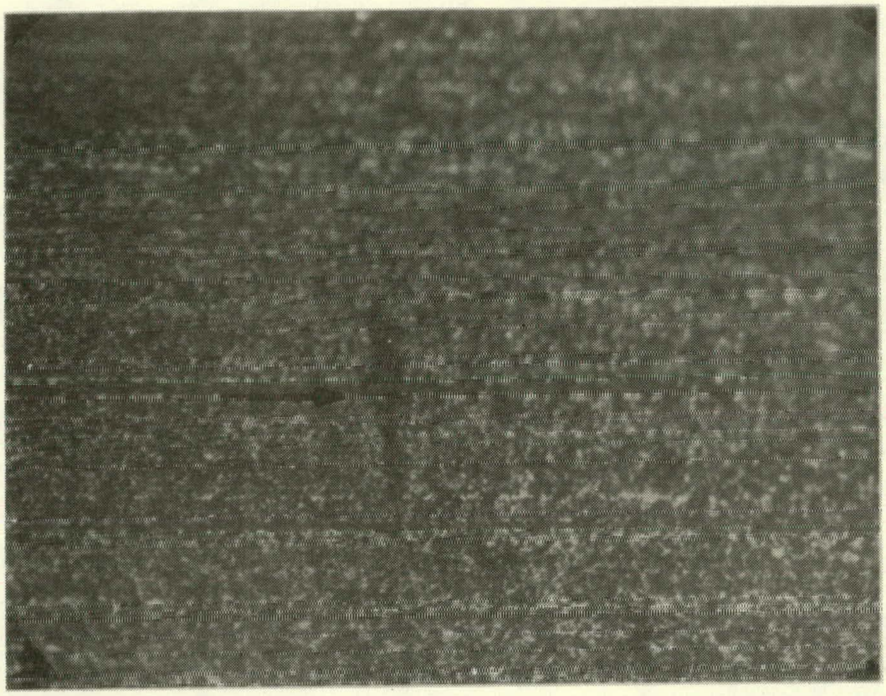

Fig. 5. Flaw Made on Surface of SiC Bar with a Knoop Indenter. The flaw is ∿ 100 μm long x 50 μm deep. 218X magnification.

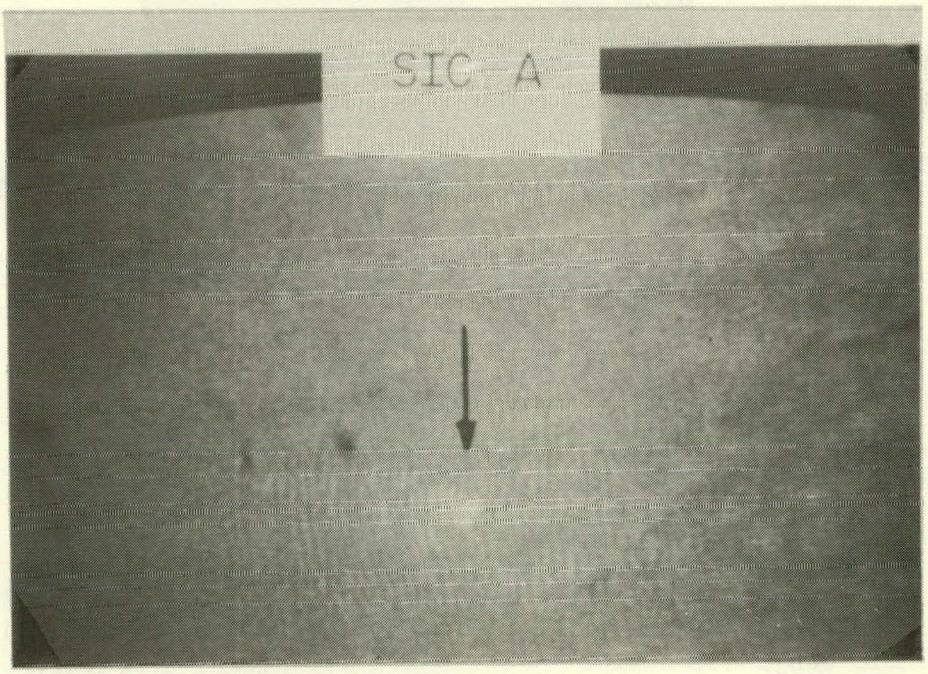

Fig. 6. Acoustic Micrograph of Surface Defect Shown in Fig. 5. Defect appears as a light area (arrow).

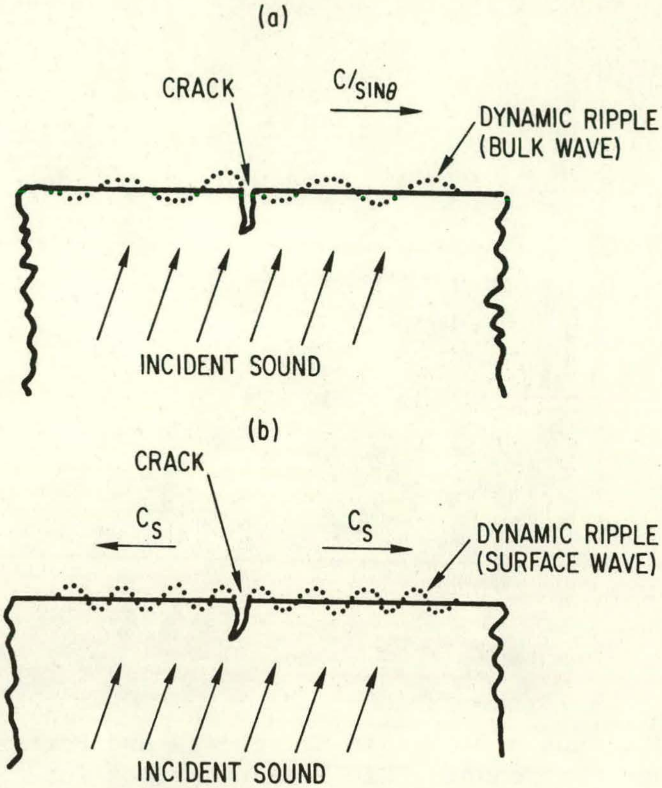

Fig. 7. Schematic Showing the Dynamic Ripples Produced by the Transmitted Bulk Wave (a) and the Wave Scattered from a Surface Flaw (b). C is the velocity of sound; θ is the angle of incidence of the beam.

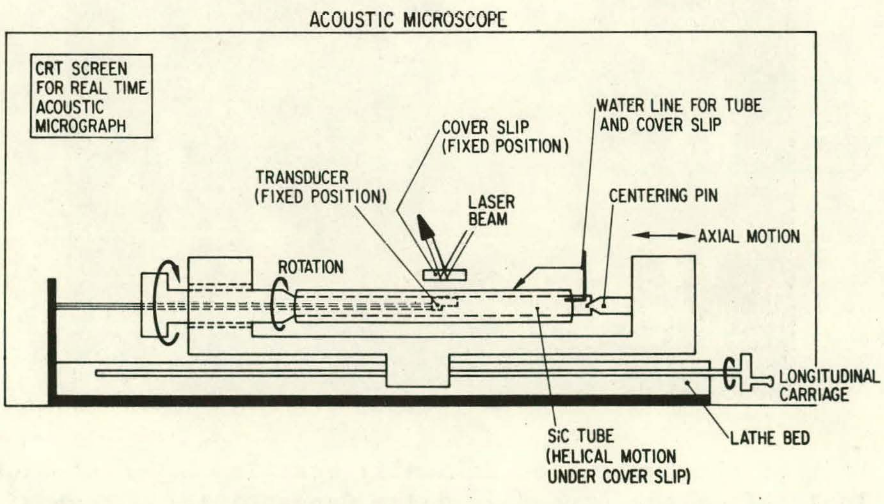

Fig. 8. Schematic of Arrangement for Carrying Out Helical Scan of SiC Heat-exchanger Tube Sections.

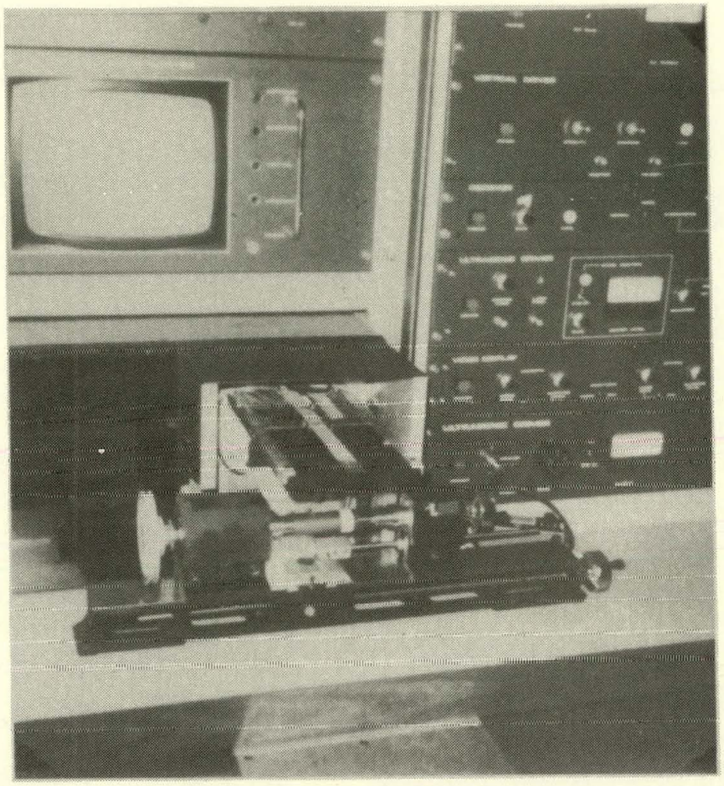

Fig. 9. Photograph of Acoustic Microscope and Partially Assembled Stage for Scanning SiC Heat-exchanger Tube Sections.

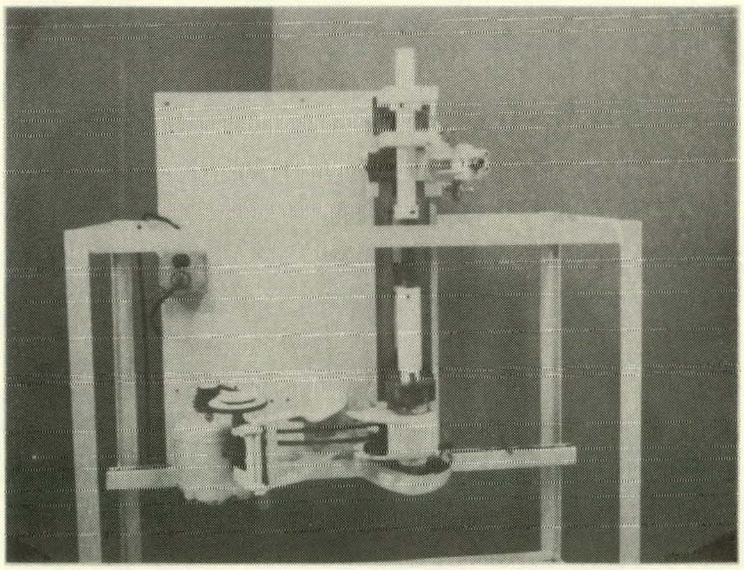

Fig. 10. Part of the System for Helically Scanning SiC Heat-exchanger Tubing from the Bore Side Using Conventional Ultrasonic Techniques.